SPE 11079

SPE
Society of Petroleum Engineers of AIME

EFFECTS OF GRID TYPE AND DIFFERENCE SCHEME ON PATTERN STEAMFLOOD SIMULATION RESULTS

by Keith H. Coats and A. Behrooz Ramesh, Intercomp Resource Development and Engineering, Inc.

This paper was presented at the 57th Annual Fall Technical Conference and Exhibition of the Society of Petroleum Engineers of AIME, held in New Orleans, LA, Sept. 26-29, 1982. The material is subject to correction by the author. Permission to copy is restricted to an abstract of not more than 300 words. Write: 6200 N. Central Expressway, P.O. Drawer 64706, Dallas, Texas 75206.

ABSTRACT

This paper presents 5-, 7-, and 9-spot pattern steamflood simulation results using parallel and diagonal grids and five-point and nine-point difference schemes. The effects of difference scheme and grid orientation are also examined in a two-dimensional (vertical) cross-section. Effects of different types of grid spacings in cyclic steam simulation are discussed. Sample problem data sets are roughly representative of a California deposit and a more viscous Alberta crude.

Various 7-spot grids (neither parallel nor diagonal) and nonuniform 5(9)-spot grids pose unique challenges to both difference schemes, with interesting results. The conclusions emphasize superiority of the nine-point difference scheme and pitfalls of certain problems/grid/difference scheme combinations used in pattern steamflood simulation.

The paper uses nine-point transmissibility alterations which allow rigorous use of 1/8 5(9)-spot patterns as opposed to 1/2 or 1/4 elements, with either parallel or diagonal grids. This is important because of significantly reduced cost compared with that of 1/4 or 1/2 pattern elements. Subject to certain conditions, the paper presents a simple procedure to calculate well productivity indices for uniform or nonuniform grids, cross-sections or any of the three patterns, and either of the two difference schemes.

BRIEF MODEL DESCRIPTION

The thermal model used here is considerably extended beyond a model previously described[1]. While the basic formulation and PVT representation are unchanged, a large number of features have been added. We will briefly discuss here only the additional features pertinent to the results presented in this paper.

The 9-point difference scheme[2] is an option in addition to the conventional 5-point scheme. This 9-point scheme is coded in the x-y planes for areal or 3D problems and in the x-z plane for two-dimensional cross-sections.

Alterations of transmissibilities necessary to run 1/8 symmetry elements of (areally) homogeneous 5- and 9-spot patterns[3] are included in the model for 5- and 9-point difference schemes with uniform or variable grid spacing.

An implicit bottomhole pressure feature[4] exactly preserves specified rates for wells not on deliverability or constraints (e.g. maximum steam production rate). For n such wells, this feature introduces n additional variables (flowing bottomhole pressure for each well) and n additional constraint equations into the matrix of equations requiring solution. This feature is coded for the 5-point D4 Gauss ordering[5], the ordinary Gauss ordering used in the 9-point scheme, and the iterative solution technique ordering.

DATA USED

The results presented below were obtained for the three data sets of Table 1. Various fluid and reservoir properties of these data sets are representative of various heavy oil deposits in the U.S. and Alberta. However, no single data set should be considered representative of any particular reservoir. Injection rate is 187.5 BPD (cold water equivalent) of steam per pattern at 400°F and 80% quality. Production rates for the pattern are reported on a full-pattern basis regardless of whether a 1/8, 1/4, 1/12, etc. pattern element is actually being simulated. Individual well production rates are similarly reported as full well rates.

Unless otherwise noted, the production wells were placed on deliverability against a flowing bottomhole pressure of 50 psia, with no maximum or limiting production rate specified. Well productivity indices in the pattern element runs were obtained as described in the Appendix and have units of RB-cp/day-psi. The simulator places appropriate multiplicative (time-varying) mobilities for all phases on these productivity indices. The relative permeability endpoints and exponents listed in Table 1 were used in analytical expressions for relative permeability[1].

Most runs were performed to 4475 days which corresponds to about 4 hydrocarbon pore volumes of steam injected, defined as Bbls of steam (CWE) injected divided by initial Bbls of hydrocarbon occupied pore space.

DESCRIPTION OF GRIDS

Fig. 1 illustrates the block-centered, parallel and diagonal grids used for symmetrical elements of repeated 5- or 9-spot patterns. Fig. 1a shows a parallel grid for 1/2 of a

References and illustrations at end of paper.

9-spot pattern. The inscribed triangle 1-2-3 is the minimal symmetrical, 1/8 pattern element. Fig. 1b shows a diagonal grid for a 1/4 9-spot pattern. The inscribed triangle 1-2-3 is the minimal 1/8 pattern element. Wells 3 and 4 in Fig. 1 are the 9-spot near-producers. If wells 3 and 4 are absent then the grids represent 5-spot pattern elements.

Fig. 2 illustrates 7-spot grids representing 1/2, 1/6, and the minimum symmetrical 1/12 elements. These symmetrical 7-spot pattern elements are obtained by noting that any straight line connecting injection wells in repeated 7-spot patterns is a line of symmetry (see Muskat[6]). In the grid of Fig. 2A, $\Delta x = 1.73205\ \Delta y$. This is necessary so that the 1/6 and 1/12 inscribed triangular elements have diagonal boundaries which intersect the rectangular blocks only at corners, resulting in simple edge block pore volume modifiers (i.e. 1/2). For the 1/2 7-spot element grid, N_y is 3N-2 where N is N_x, the number of grid blocks in the x-direction.

The square pattern elements of Figs. 1 and 2 are the smallest pattern elements of symmetry (for the grid orientations used) which avoid diagonal boundary lines. Simulation of the parallel and diagonal 1/8 9- or 5-spot pattern elements shown in Fig. 1 gives results identical to those obtained by simulating the corresponding 1/2 and 1/4 pattern elements. This is true for both the 5-point and 9-point difference schemes. Use of the 1/8 as opposed to the 1/2 or 1/4 elements reduces computing costs appreciably[3]. Simulations of the 1/12 or 1/6 7-spot elements of symmetry do not agree with results from simulation of the 1/2 pattern element as shown below.

Table 2 summarizes grid characteristics for the three minimal grids (1/8 parallel, 1/8 diagonal and 1/12 7-spot). The term d is distance (feet) between injector and producer (far producer in 9-spot case). N is the number of grid blocks in the x-direction and A is full pattern acreage.

Table 3 shows the number of x-direction grid blocks (N) which the diagonal grid must have to give the same block dimensions as the parallel grid for the 5(9)-spot pattern. Active block numbers are for the 1/8 pattern grid. This table shows that nearly equal block sizes occur in comparisons of 8x4 parallel to 6x6 diagonal grid results and 11x6 parallel to 8x8 diagonal grid results. 11x6 parallel and 8x8 diagonal 5(9)-spot grids will be denoted as "equivalent" grids below. This term "equivalent" simply denotes roughly equal grid block dimensions.

GRID ORIENTATION EFFECTS IN 5-SPOT AND 9-SPOT SIMULATIONS

The 5-point difference scheme conventionally used in numerical simulation can introduce significant disparity in results for equivalent parallel and diagonal grids. This disparity was noted by Todd et al[7] for adverse mobility ratio waterfloods and later by Coats[8] for steamfloods. Abou-Kassem and Aziz[9] report a detailed comparison of the 9-point difference and other numerical schemes as remedies to the grid orientation problem in 1/4 of a 5-spot steamflood pattern. They conclude that the 9-point scheme significantly reduces the grid orientation effect.

Steamflood simulation Runs 1-4 were performed with Data Set 1 for 1/8 of a 2.5 acre 5-spot, using 5- and 9-point difference schemes, and parallel and diagonal grids. Runs 1 and 2 used 8x8 diagonal grids with the 9- and 5-point schemes, respectively. Runs 3 and 4 used 11x6 parallel grids with 9- and 5-point schemes, respectively.

The 5-point scheme Runs 2 and 4 calculated steam breakthrough times of 2530 and 750 days for the diagonal and parallel grids, respectively. The 9-point scheme Runs 1 and 3 gave breakthrough times of 1490 and 1700 days, respectively. Figures 3 and 4 compare full pattern oil rate and recovery vs. time for these four runs. The results indicate that the 9-point difference scheme significantly reduces the grid orientation effect.

The smallest symmetry element of the 9-spot pattern includes an injection well 1, a far producer 2, and a near producer 3, shown in Fig. 1. Depending on the choice of grid type, either well 2 or well 3 has a diagonal connection with the injector.

Runs 5 and 6 simulated 1/4 of a 9-spot using the 5-point difference scheme in 11x6 parallel and 8x8 diagonal grids, respectively. Runs 7 and 8 are the same as Runs 5 and 6 except that the 9-point scheme was used. For Runs 5 and 6, Figure 5 shows that with the conventional 5-point scheme, the breakthrough sequence of the far and near producers is reversed by using parallel and diagonal grids. Figure 6 presents an equally confusing picture of recovery for the two producers with parallel and diagonal grids.

The 9-point Runs 7 and 8, on the other hand, calculate consistent behavior for both wells, regardless of the type of grid used as shown in Figures 7 and 8.

RESULTS WITH AN OFF-CENTER WELL

The above results were obtained for uniform grid spacings with square grid blocks. All lines connecting injection-production wells were at angles of either 0 or 45 degrees to the x- or y-axis. The 9-point scheme (for square grid blocks) adds flow terms at 45 degrees to these coordinate axes. The question therefore arises as to the ability of the 9-point scheme to reduce grid orientation effects in cases with injection-production well lines between 0 and 45 degrees to the x(y)-axis.

Fig. 9 shows 11x11 and 15x8 diagonal and parallel grids for 1/8 of a 5-spot with an additional production well located as shown. The full pattern includes eight of these added production wells, and we report here the calculated, full-pattern oil recovery from these eight wells. The added well locations, as represented by the distances from the diagonal noted on Fig. 9, are not exactly the same for the two grids. For the diagonal grid, ℓ is 1.05 times that of the parallel grid.

Figs. 10 and 11 show calculated pattern oil recovery and rates from the added wells for Runs 9-12 using the four combinations of diagonal vs. parallel grid and 5-point vs. 9-point difference schemes. For the diagonal and parallel grids, the 5-point scheme gives steam breakthrough times (at the added well) of 336 and 556 days, respectively. For the same two grids, the 9-point scheme gives breakthrough times of 471 and 451 days, respectively. Peak oil rates for the 5-point scheme are 481 and 629 STB/day for the two grids. The peak rates for the 9-point scheme are 804 and 787 STB/D. Thus the 9-point scheme virtually eliminates effect of grid orientation in this case of a production well located between 0 and 45 degrees to the x-axis.

The magnitude of grid orientation effect and its elimination by the 9-point scheme were unaffected by changing the initial water saturation from 27% in the above runs to 35% (S_{wir} = 35%).

The runs were also repeated (with S_{wi} = .27) with the added well located in grid block I=8, J=4 for both grids. The diagonal grid ℓ value (see Figure 9) is .933 times the parallel grid ℓ value. In this case all four runs give virtually identical steam breakthrough times and oil rates for the added well.

That is, no grid orientation effect appeared for the 5-point scheme.

EFFECT OF RECTANGULAR GRID BLOCKS

The above results used square grid blocks. Here we use a grid of rectangular grid blocks with $\Delta x = 2\Delta y$ and examine the response of the two (identical) near producers in 1/4 of a homogeneous 2.5 acre 9-spot. Data set 1 was used with upstream convective weighting and the 9-point difference scheme. The results of Runs 13-16 are summarized in Table 4 and shown in Fig. 12.

Table 4 shows that Run 15, using the 2:1 rectangular blocks, gives almost a 5-fold difference in steam breakthrough times at the two identical near-producers 3 and 4. Also, the cumulative oil and total liquid recovery at 4475 days (3.95 PV steam injected) is over twice as large for the near producer well 3. Figure 12 shows the disparity in cumulative oil recovery for the two symmetric wells of a 1/4 of 9-spot using 5x9 rectangular grid compared with identical results for the same two wells in an 8x8 square grid.

This disparity is neither a consequence of nor remedied by choice of difference scheme. We felt the different breakthrough times might reflect primarily the different total pore volumes (which must be heated to steam temperature) in the single rows of 5 and 9 blocks connecting the injector to wells 3 and 4, respectively. The pore volume of the row connecting the injector to well 3 is 1/2 that to well 4 for this case of $\Delta x = 2\Delta y$. However, a nearly identical disparity of well 3 vs. well 4 performance occurred when we used $\Delta x_1 - \Delta x_5 =$ 20.625, 30.9375, 41.25, 41.25, 82.5 feet, which gives identical injector-near producer total row pore volumes for both wells 3 and 4. Results were also unaffected by using midpoint convective weighting. Use of more grid blocks (9x16 grid) gave a disparity very close to that of Run 15.

These results indicate that in the homogeneous case, production wells placed symmetrically to an injector must "see" an identical grid/transmissibility path in order to respond identically. In the case of a 9-spot this translates to the necessity of square grid blocks or identical variable grid spacings in the x- and y- directions.

One factor which aggravates the disparity exhibited in Run 15 is the placement of production wells on deliverability with no limit on total well production rate. Once a mobile finger nears and breaks through at one well, the unlimited, very large fluid withdrawal from that well "short-circuits" the pattern, virtually shutting off continued fluid/heat flow toward the symmetrical other producer. Fig. 13 indicates this effect.

Run 16 is the same as Run 15 except that the production wells are limited to 200 RB/D total liquid production rate to reduce the above mentioned effect. As shown in Table 4 and Fig. 14, the breakthrough times are nearly identical for the two near-producers and the disparity in total liquid production at 4475 days is reduced significantly.

One might question whether disparities similar to that of Run 15 might occur with square grid blocks if perturbed permeability and/or initial saturation distributions favor flow toward one of the two near producers. We have observed the same qualitative effect resulting from such heterogeneities. However, use of square blocks with 50% reduced permeability or increased initial S_w (from .27 to .37) between one injector-producer gave disparities significantly less than that of Run 15. That is, the distortion caused by the 2:1 grid block aspect ratio in the 9-spot case appears to be a very strong distortion compared with those caused by moderate heterogeneity or initial saturation irregularities.

7-SPOT RESULTS

Runs were performed using Data Set 1 for the 1/2, 1/6 and 1/12 7-spot grids shown on Fig. 2. The 1/2- and 1/6- 7-spot grids exhibit both diagonal and parallel injector-producer flow paths. The 1/12 7-spot element grid exhibits a diagonal injector-producer connection.

Fig. 15 compares well 2 cumulative oil recovery vs time for the 1/2 7-spot (5x13) and 1/12 7-spot (5x5) grids using 5-point and 9-point difference schemes. The 1/12 and 1/2 element results do not agree for either difference scheme. The difference between 1/2 and 1/12 element results is significantly less for the 9-point as opposed to 5-point difference scheme.

The 1/6 7-spot element (Fig. 2b) with a 9x5x1 grid exhibits diagonal and parallel injector-producer paths to symmetrical wells 2 and 3, respectively. Obviously wells 2 and 3 should behave identically. Figs. 16 and 17 show well 2 and 3 response for the 1/6 7-spot 9x5 grid using 5-point and 9-point difference schemes. For the 9-point difference scheme, well 2 (with diagonal connection) breaks through at 786 days compared to 2819 days for well 3. The opposite extreme occurs in the 5-point difference with well 2 breaking through at 3540 days compared to 660 days for the (parallel-connection) well 3. These wide differences in breakthrough time are aggravated by the short-circuiting effect associated with unlimited well production rate, mentioned earlier.

The 1/6 7-spot results shown in Figs. 16 and 17 were recomputed using a total liquid production rate limit of 200 RB/D for each production well. Figs. 18 and 19 show the results with this limiting rate imposed. The differences between wells 2 and 3 breakthrough times and recoveries are significantly reduced and the two wells behave more similarly for the 9-point than the 5-point difference scheme.

EFFECTS OF PATTERN TIP BLOCK ELIMINATION

The grids shown in Figs. 1 and 2 result in small tip blocks with wells located in at least two of them. Past experience showed the 5-spot well tips could be eliminated in parallel grids using the 5-point difference scheme. Absorbing the volumes of the tip blocks into their neighboring blocks for that case resulted in less computing time and little difference in results.

Here we examine the effect on 5-spot pattern results of tip block elimination using the more accurate 9-point difference scheme and parallel and diagonal grids. The base Runs 25 and 26 use equivalent 6x6 diagonal and 8x4 parallel grids with no tip elimination. Runs 27 and 28 use the same diagonal and parallel grids, respectively, with the well tip blocks eliminated. Data Set 1 was used.

Fig. 20 compares cumulative oil production vs time for the 4 runs. The results are plotted for a reduced portion of the total 4475-day runs to emphasize the differences in results. Fig. 20 shows that the effect of tip elimination is small for the diagonal grid but is significant for the parallel grid.

The reason for considering tip elimination is evidenced by the reduction in Harris 800 computing time from 161 CPU seconds in Run 25 to 112 in Run 27. For 3D pattern grids including a number of layers, these times can be considerably larger and the cost savings due to tip elimination can be important in a study involving many runs.

Runs 27 and 28 used the same production well indices (28.9 and 28.8 RB-cp/day-psi, respectively) as were used in

Runs 25 and 26. The method described in the Appendix was used to determine the correct productivity indices of 25.1 and 25 RB-cp/da-psi, for Runs 26 and 27, respectively. Run 27 and 28 results were unaffected by this 13% reduction in productivity index.

Run 28 was repeated with all four tip blocks removed rather than just the two well tip blocks. The effect on results was small.

These results indicate that tip elimination may be justifiable in diagonal grids but questionable in parallel grids in pattern calculations using the 9-point difference scheme.

GRID ORIENTATION EFFECTS IN X-Z CROSS-SECTIONS

The above results relate to effects of grid orientation in the x-y or areal plane. This section shows the sensitivity of cross-sectional steamflood results to grid-orientation in the vertical x-z plane.

The reservoir-fluid data for Runs 29-34 are given in Data Set 2 of Table 1. The cross-section is 300 feet long, 120 feet thick and 40 feet wide. Permeability and porosity are 5500 md and .33, respectively, and the dead oil viscosity ranges from 3720 cp at 100°F to 6.28 cp at 400°F. Initial water saturation of .37 compares with the irreducible water saturation of .2.

Runs 29-30 and 33-34 use a normal, "parallel" 15x6 grid with $\Delta x = \Delta z = 20$ feet for each grid block. A roughly equivalent "diagonal" 14x14 grid, shown on Fig. 21, was used in Runs 31 and 32. The grid blocks are 21.21 feet square. The appropriate edge grid blocks are halved and external grid blocks are zeroed. All nonzero pore volumes and transmissibilities are calculated with the x-axis horizontal as shown, and then the entire plane is rotated at a 45° dip angle. Heat loss is zero for all runs, and injection and production occur in the single lowermost left and lowermost right grid blocks, respectively.

If the 5-point internal transmissibilities are 1.0, then for the 9-point scheme in the Fig. 21 diagonal grid the internal x- and y- direction transmissibilities are 2/3, the internal diagonal transmissibilities are 1/6 and the edge diagonal transmissibilities (parallel to the edge) are 1/12.

Fig. 22 compares cumulative oil recovery vs time for Runs 29-32. The results differ somewhat but are generally close for all cases. For a given difference scheme, recovery is somewhat higher for the parallel grid than the diagonal grid. For a given grid, the 9-point scheme gives higher recovery than the 5-point scheme.

Some Truncation Error Observations

Runs 29-32 were performed using .5 or arithmetic mean weighting on the convective heat interblock flow terms and using a maximum saturation change of .1 for time step control. Run 33 is the same as Run 29 except that full upstream weighting (ω=1.0) was used for the convective heat flow terms. Run 34 was the same as Run 29 except that a time step control of .25 saturation change per step was used.

Fig. 23 compares Runs 29, 33 and 34 in oil recovery vs time. The effect of .5 vs 1.0 upstream heat flow weighting (Run 29 vs. Run 33) upon oil recovery is greater than the effects of any of 5-point vs 9-point and parallel vs diagonal grids in Runs 29-32. We have generally observed that midpoint convective weighting (ω=.5) gives more accurate steamflood results.

Fig. 23 shows that the increased time step size of Run 34 had little effect. The time steps, outer iterations and computing times for Runs 29, 33 and 34 are as follows:

Run	Time Steps	Iterations	Harris 800 CPU Seconds
29	205	1044	3251
33	200	921	2950
34	93	619	1921

Run 29 (.1 saturation control) required 69% more computing time than Run 34 (.25 saturation control) with essentially no difference in results. These results indicate the cost saving potential of fully implicit formulations. However, the user should be aware that fully implicit formulations are capable of taking time step sizes above the point at which time truncation error arises.

GRID EFFECTS IN SINGLE WELL STIMULATION

This problem concerns sensitivity of cyclic steam stimulation runs to radial grid spacing. Since this spatial truncation error is not reduced by refinement of the z-direction grid spacing, we will illustrate the problem and a remedy with one-dimensional radial results.

Data Set 3, listed in Table 1, describes a 3700 md, 80-foot formation with an oil viscosity of over five million cp at the original reservoir temperature of 55°F. The initial mobile water saturation of .2 compares with an irreducible water saturation of .1. Initial gas saturation is zero, and the oil is a dead oil.

This problem was presented to us together with the following comments: "Calculated oil recovery differs significantly as 8, 12, and 20 grid blocks are used. Use of more grid blocks is no help since use of more than 20 blocks results in loss of steam injectivity due to reservoir pressurization. The calculated steam injected over the 40-day injection period falls increasingly below the actual field rate of 1,000 BPD. Estimated bottomhole flowing pressure during field injection never exceeded 700 psia. With more than 20 blocks, a bottomhole pressure limit of 1500 psia failed to sustain a calculated rate of 1,000 BPD for 40 days." An effective formation compressibility of .0002 psi^{-1} was used in the results referred to in the latter comments.

Single-well studies, whether isothermal coning or steam stimulation, are normally performed using a geometrically spaced radial grid with $r_i = \alpha r_{i-1} = \alpha^2 r_{i-2}$, etc. This results in a rapidly increasing grid block size, Δr, with increasing distance from the well. This larger "remote" radial spacing causes little truncation error in problems such as black oil coning where saturation and pressure gradients are sharp only near the well and rather flat away from the well.

However, this single-well geometric grid can cause serious truncation error for any stimulation process which involves sharp pressure/saturation/temperature/composition gradients which move significantly deep into the reservoir. Patton and Coats[10] noted the inadequacy of the geometric grid in numerical studies of isothermal CO_2 stimulation of heavy oil wells.

Steam stimulation can produce sharp temperature, pressure, and saturation gradients as heated oil is pushed away from the well into cold regions. While the resulting "oil bank" formation is most pronounced in reservoirs having an initially mobile water saturation, the immobile oil banks can also form in a multi-cycle stimulation of a reservoir initially containing irreducible water saturation.

The "correct" results in the set referred to in the above comments are those corresponding to a large number of blocks. That is, for the given fluid and rock properties, an injection rate of 1,000 BPD for 40 days cannot be sustained. The 8- and 12-block simulations attained the observed injection rate (using a 1,500 psia pressure limit) only due to excessive spatial truncation error. As more blocks were used and truncaton error decreased, the correct answer of insufficient injection capacity appeared.

A number of possible data errors might explain this disparity between observed and calculated injectivity. For example, an undetected initial gas saturation might be present, relative permeability curves might be significantly in error, actual bottomhole steam quality might be lower than specified in the calculations and/or effective formation compressibility might be significantly greater than .0002 psi^{-1}.

As the choice of "remedy" is immaterial to the truncation error problem here, we adopted the simplest remedy of an effective formation compressibility of .0015 psi^{-1}, which resulted in sustained injectivity with pressures below 700 psia. With compressibilities this large, it is important to use the exponential as opposed to linearized expression for pore volume in the simulator.

Eight simulation runs were performed for the two stimulation cycles. Runs 35-37 used geometric spacing with 8, 12, and 20 radial grid blocks, respectively, and a first block center radius of 2 feet. Runs 38-42 used various numbers of equal-volume radial blocks within a radius of 90 feet and with geometrically-spaced blocks from 90 to 650 feet.

The radius of 90 feet was determined as a value somewhat larger than the deepest penetration of sharp gradients into the reservoir during second-cycle injection and production. This radius must be determined by calculations for each problem and will be larger for more cycles for a given problem.

The calculated oil/steam ratios STB/Bbl(CWE) for each cycle for these runs are given in Table 5. Cumulative oil recoveries are shown in Fig. 24. These results show the significant truncation error or grid sensitivity in the geometric grid, Run 35-37 results. Runs 38-41 agree rather closely by individual cycle and even more closely in total oil recovered from both cycles. Run 41 indicates that only 1 grid block may be necessary outside the radius of influence.

Fig. 25 shows the extremely sharp profiles between 60 and 85 feet as calculated from the 23-block Run 38. The Run 38 grid includes 10 grid blocks between 62 and 87 feet. The 20-block, geometric Run 35 grid has only <u>one</u> grid block spanning 61-82 feet.

The use of equal-Δr blocks, as opposed to equal-volume blocks, within the first 90 feet from the well also gives good results. Figure 25 compares Runs 38 and 43 representing equal-volume and equal-Δr grid spacing, respectively.

SUMMARY

Large grid orientation errors can result from use of the conventional 5-point difference scheme in simulation of 5-spot and 9-spot pattern steamfloods. For 9-spot patterns, the 5-point scheme can give steam breakthrough at the far producer earlier than at the near producer. With the use of square areal grid blocks, the 9-point difference scheme significantly reduces the grid orientation effect.

This greater accuracy of the 9-point scheme also seems to hold when production wells are located between the coordinate axes and the 45° line.

The use of non-square (2:1 aspect ratio) grid blocks, with production wells on deliverability, in a 1/4 9-spot simulation resulted in a large grid orientation error for both 9-point and 5-point schemes. When each production well total rate was limited in order to reduce a short-circuiting effect, the 9-point scheme gave a much smaller grid orientation effect.

While neither difference scheme gives the same results for the rectangular 1/2 and triangular (element of symmetry) 1/12 7-spot grids, the 9-point results agree more closely than the 5-point results.

Grid orientation effects in the vertical plane were examined by comparing cross-sectional results for parallel and diagonal grids and both difference schemes. Results for all four combinations showed some differences one-to-another. However, the differences were significantly less pronounced than those of areal pattern calculations.

Cyclic steam stimulation results were calculated for a very heavy oil using the conventional geometrically-spaced grid and an equal cell-volume grid. The results indicate that significant error resulting from geometric radial spacing can be virtually eliminated with equal-volume spacing. Comparably good results were also obtained using equal Δr spacing.

The Appendix presents a relatively simple procedure for obtaining pattern or cross-section well indices for the 5- or 9-point difference scheme.

NOMENCLATURE

A	acres per pattern
d	distance between pattern injector and producer, ft.
h	formation thickness, ft.
k	permeability, md
k_{ro}	relative permeability to oil
k_{rw}	relative permeability to water
k_{rg}	relative permeability to gas
N, N_x	number of grid blocks in x-direction
N_y	number of grid blocks in y-direction
$n_w, n_{ow}, n_{og} n_g$	analytical relative permeability curve exponents
p	pressure, psia
PI	well productivity index, RB-cp/day-psi
q	well injection or production rate
r_w	wellbore radius, ft.
S	fluid saturation, fraction
S_{wir}	irreducible water saturation
S_{orw}	residual oil saturation to water
S_{org}	residual oil saturation to gas
w	width of cross-section or distance between like wells in direct line drive, ft.

Greek

λ	mobility, relative permeability/viscosity, 1/cp

μ	viscosity, cp
ω	upstream weighting factor for convective heat flow (ω=1.0 is full upstream)

Subscripts

wb	wellbore
1	injection
2	production

REFERENCES

1. Coats, K.H.: "A Highly Implicit Steamflood Model," Soc. Pet. Engr. J. (Oct. 1978) 369-383.
2. Yanosik, J.L., and McCracken, T.A.: "A Nine-Point, Finite-Difference Reservoir Simulator for Realistic Prediction of Adverse Mobility Ratio Displacements," Soc. Pet. Engr. J. (Aug. 1979) 253-262.
3. McDonald, A.E., and Trimble, R.H.: "A Strongly Coupled, Fully Implicit, Three-Dimensional, Three-Phase Well Coning Model," Soc. Pet. Engr. J. (Aug. 1981)454-458.
4. Coats, K. H., "Simulation of 1/8 5(9)-Spot patterns", SPEJ Forum, under current review by SPE, August, 1982.
5. Price, H.S., and Coats, K.H.: "Direct Methods in Numerical Simulation," Soc. Pet. Engr. J. (June 1974) 295-308.
6. Muskat, Flow of Homogeneous Fluids through Porous Media, J.W. Edwards, Inc., Ann Arbor, Michigan, 1946.
7. Todd, M.R., O'Dell, P.M. and Hirasaki, G.J.: "Methods for Increased Accuracy in Numerical Reservoir Simulators," Soc. Pet. Engr. J. (Dec. 1972) 515.
8. Coats, K. H., George, W. D., Chu, Chieh, and Marcum, B. E., "Three-Dimensional Simulation of Steamflooding", Soc. Pet. Eng. J. (Dec. 1974) 573-592; Trans., AIME (1974, 157.
9. Abou-Kassem, J. H. and Aziz, K., "Grid Orientation During Steam Displacement", SPE 10497 presented at the Sixth SPE Symposium on Reservoir Simulation, New Orleans, La., Feb. 1-3, 1982.
10. Patton, John T. And Coats, Keith H.: "A Parametric Study of the CO_2 Huff-n-Puf Process," paper SPE 9228 presented at the SPE 54th Annual Meeting, Las Vegas, September 23-26, 1979.
11. Peaceman, D.W.: "Interpretation of Well-Block Pressures in Numerical Reservoir Simulation," Soc. Pet. Engr. J. (June 1978) 183-194.
12. Peaceman, D. W., "Interpolation of Well Block Pressures in Numerical Reservoir Simulation with Non-Square Grid Blocks and Anisotropic Permeability", SPE 10528 presented at the Sixth SPE Symposium on Reservoir Simulation, New Orleans, La., Feb. 1-3, 1982.
13. Hillestad, J.G. and Kuniansky, J.: "Reservoir Simulation Using Bottomhole Pressure Boundry Conditions," Soc. Pet. Engr. J. (Dec. 1980) 473-486.

APPENDIX
CALCULATION OF WELL PRODUCTIVITY/INJECTIVITY INDICES FOR PATTERNS AND CROSS-SECTIONS

Peaceman[11,12] and Hillestad[13] present detailed mathematical developments for productivity indices of wells in numerical simulations. They point out the principle of using the simulator itself in determining well indices. We utilize that principle here. They show that the indices depend upon grid block size and shape, adjacent grid block spacings, location of the well within the block, boundary conditions on the block edges and the difference scheme (5-point vs 9-point) employed.

A simple procedure accounting for all these factors can be used to calculate the indices for certain 5-, 7- and 9-spot patterns and cross-sectional cases. Areal homogeneity, steady-state flow and fully penetrating wells are assumed. Muskat[6] gives index reduction factors for partial penetration cases. Alternatively, as a rough approximation, the full penetration procedure described here can be used to generate indices for each layer in stratified reservoirs having areally homogeneous layers of differing permeability and thickness.

We first consider the case of 5-, 7- or 9-spot patterns. The x-y (areal) grid spacing may be variable but is restricted to symmetry about the injection and production wells. The 9-spot well indices are assumed to be identical or close to those of the 5-spot so only the 5- and 7-spot patterns are considered. The procedure described here assumes the areal grids shown in Figs. 1 and 2. However the procedure is applicable to determination of the well indices for $\Delta x \neq \Delta y$, variable areal spacing, for the case of eliminated tip (well-block) grid blocks and for the 5-point or 9-point differ-ence schemes.

Muskat gives the 5- and 7-spot steady state, single-phase flow conductivities. His equations can be rearranged to the forms:

$$p_{wb1} - p_{wb2} = \frac{q\mu}{kh} \frac{\ln(d/r_w) - .6190}{\pi} \quad (1)$$

$$p_{wb1} - p_{wb2} = \frac{q\mu}{kh} \frac{3\ln(d/r_w) - 1.7073}{4\pi} \quad (2)$$

for the 5-spot and 7-spot, respectively. q is production rate for a single pattern, subscripts 1 and 2 refer to injection and production wells, respectively, and d is the distance from injector to producer. Rearrangement of these equations gives

$$\frac{q}{kh\lambda\Delta p} = \frac{\pi}{\ln\frac{d}{r_w} - .6190} \quad \text{5-spot} \quad (3)$$

$$\frac{q}{kh\lambda\Delta p} = \frac{4\pi}{3\ln\frac{d}{r_w} - 1.7073} \quad \text{7-spot} \quad (4)$$

Where Δp is injector-producer wellbore pressure difference, q is single-pattern rate, and λ is the (single) flowing phase mobility. The numerical simulator can be run in single-phase mode for a few time steps to generate a stabilized flow rate

q and injection and production well grid block pressures p_1 and p_2. The run can be performed with the wells on deliverability (injectivity) with arbitrary limiting flowing bottomhole pressures and well indices. If a symmetrical element of a single pattern is used (e.g. 1/8 5-spot) then the simulator rate should be scaled to a full pattern (e.g. multiplied by 8). A single pattern is arbitrarily defined here as including one injector. The 5-spot pattern then has 1 producer while the 7-spot pattern has 2 producers.

Due to the linearity of the single-phase flow equation, the simulator results obey the following equations:

$$q = \alpha k h \lambda (p_{wb1} - p_1) \quad (5a)$$

$$q = \beta k h \lambda (p_1 - p_2) \quad (5b)$$

$$q = n\alpha k h \lambda (p_2 - p_{wb2}) \quad (5c)$$

where n is the number of producers per pattern. These equations can be combined (isolate the pressure differences by division and add the equations) to yield:

$$\frac{q}{kh\lambda \Delta p} \left(\frac{n+1}{n\alpha} + \frac{1}{\beta}\right) = 1 \quad (6)$$

where Δp is $p_{wb1} - p_{wb2}$. Comparison of Eqns (3) and (4) with Eqn (6) gives:

$$\alpha = \frac{(n+1)/n}{\frac{\ell n\,(d/r_w) - .6190}{\pi} - \frac{1}{\beta}} \quad \text{5-spot} \quad (7)$$

$$\alpha = \frac{(n-1)/n}{\frac{3\,\ell n\,(d/r_w) - 1.7073}{4\pi} - \frac{1}{\beta}} \quad \text{7-spot} \quad (8)$$

The value of β is obtained from simulator results using Eqn (5b) as:

$$\beta = q/.001127kh\lambda(p_1 - p_2)$$

where units of RB/d, md, ft, cp and psi are used. The value of α is then calculated from Eqn (7) or (8) and the injection (production) well index is:

$$PI = .001127\ \alpha kh\ \frac{RB\text{-}cp}{day\text{-}psi} \quad (9)$$

for any kh value, in md-ft.

The well productivity index for use in cross-sectional calculations can be calculated simply provided a number of assumptions are made. The cross-section of constant width w and thickness h is identified with a symmetrical element of a repeated direct line drive pattern with distances d and w between unlike and like well-pairs, respectively. The injector and producer in the cross-section are centered in the width, located at the ends (faces) x=o and x=d, and fully penetrate the thickness. Steady-state, single-phase flow and uniform horizontal permeability are assumed. In the numerical calculation, the grid points (subscripts) 1 and 2 referred to below are located at the injection (x=o) and production (x=d) faces of the cross-section.

For the repeated direct line drive pattern, Muskat gives for steady, single-phase flow,

$$p_{wb1} - p_{wb2} = \frac{q\mu}{kh}\left(\frac{d}{2w} - \frac{1}{\pi}\,\ell n\,\frac{2\pi r_w}{w}\right) \quad (10)$$

A numerical calculation at steady-state will give:

$$p_1 - p_2 = \frac{q\mu}{kh}\,\frac{d}{2w} \quad (11)$$

for any (uniform or variably-spaced) x-direction grid.

Subtraction of Eqn (11) from Eqn (10) and rearranging gives:

$$q = \frac{2\pi}{\ell n(2\pi r_w/w)}\,\frac{kh}{\mu}\,(p_{wb} - p)_i \quad (12)$$

where i is 1 or 2 and q is total well injection rate. Thus in engineering units of RB/D for q, md for k, cp for μ, and feet for distances, the productivity (injectivity) index for a full well is:

$$PI = \frac{.007084}{\ell n(2\pi r_w/w)}\,\frac{kh}{\mu}\,\frac{RB\text{-}cp}{day\text{-}psi} \quad (13)$$

The cross-sectional numerical calculation should utilize 1/2 of this index since the cross-section includes 1/2 of an injector, 1/2 of a producer and flow rate is 1/2 of a total well's rate. For a fully penetrating well in a cross-section having layers of differing permeability, we use Eqn (13) with layer values entered for kh. Muskat gives charts showing the effect of partial penetration on well indices, but this becomes involved in layered cross-sectional cases.

TABLE 1

RESERVOIR FLUIDS AND ROCK DATA USED

	Data Set 1	Data Set 2	Data Set 3
OIL PROPERITIES:			
stock tank density, lb/ft^3	60.3	62.0	62.1
viscosity, cp, @ ^oF	1380@100	3720@100	$5.1x10^6$@55
viscosity, cp, @ ^oF	3@400	6.3@400	6.5@455
compressibility, psi^{-1}	.00001	.000005	.0000055
expansion coefficient, $^oF^{-1}$	.0004	.00038	.00038
specific volume at initial reservoir P and T, ft^3/lb	.01658	.01560	.01610
oil molecular weight	338.6	380.	400.
ideal gas state heat capacity Btu/lb^oF	.35	.50	.48
solution gas or distillable component	0	0	0
ROCK PROPERTIES:			
thickness, feet	50	120	80
permeability, md	2000	5500	3700
porosity, percent	30	33	32
effective compressibility, psi^{-1}	.0005	.0003	.0016
irreducible water saturation, S_{wir}	.25	.2	.10
residual oil to water, S_{orw}	.2	.25	.32
residual oil to gas, S_{org}	.05	.15	.15
critical gas saturation, S_{gc}	.04	0	.02
residual gas saturation, S_{gr}	.04	0	.02
k_{ro} @ S_{wir}	.5	1.0	1.0
k_{rw} @ S_{orw}	.28	.025	.15
k_{rg} @ $S_{wir} + S_{org}$	.5	.4	.2
n_w	3.0	3.0	5.0
n_{ow}	2.3	1.4	1.3
n_{og}	3.2	1.7	2.6
n_g	1.7	1.3	2.3
capillary pressure	0	0	0
INITIAL CONDITIONS:			
pressure, psi	100	240	250
temperature, ^oF	100	100	55
water saturation	.27	.37	.2
gas saturation	0	0	0

TABLE 2

GRID CHARACTERISTICS FOR MINIMAL ELEMENTS OF SYMMETRY

PATTERN-GRID	d	N_y	Δx	Δy	ACTIVE BLOCKS
1/8 5(9)-SPOT, DIAGONAL	$\sqrt{21780A}$	N	$(d/\sqrt{2})/(N-1)$	Δx	$N(N+1)/2$
1/8 5(9)-SPOT, PARALLEL	$\sqrt{21780A}$	N/2*	$d/(N-1)$	Δx	$N(N+2)/4$**
1/12 7-SPOT	$\sqrt{16766.2A}$	N	$1.73205\,\Delta y$	$.5d/(N-1)$	$N(N+1)/2$

*If N is odd, round up, e.g. if N=7, N_y=4.

**If N is odd, active blocks are $(N+1)^2/4$.

TABLE 3

EQUIVALENT PARALLEL-DIAGONAL GRIDS IN 5(9)-SPOT PATTERNS

PARALLEL GRID		DIAGONAL GRID		
N	ACTIVE BLOCKS	N	ACTIVE BLOCKS	ROUNDED N
5	9	3.83	10	4
7	16	5.24	15	5
8	20	5.95	21	6
11	36	8.07	36	8
14	56	10.19	55	10
15	64	10.9	66	11

TABLE 4

EFFECT OF RECTANGULAR GRID BLOCKS ON 1/4 9-SPOT RESULTS

		STEAM BREAKTHROUGH TIME, DAYS		CUMULATIVE PRODUCTION (MSTB) WATER		OIL	
RUN	GRID	WELL 3	WELL 4	WELL 3	WELL 4	WELL 3	WELL 4
13	8x8	600	600	383	383	54	54
14	5x5	516	516	373	373	53.2	53.2
15	5x9	435	1951	541	237	77.5	30.6
16*	5x9	850	870	426	349	58.1	47.6

* Production wells on 200 RB/D total liquid limit.

TABLE 5

SUMMARY OF SINGLE WELL STIMULATION RESULTS

RUN	CUMULATIVE OIL/STEAM CYCLE 1	CUMULATIVE OIL/STEAM CYCLE 2	SPACING	BLOCKS
35	.264	.150	Geometric	8
36	.22	.424	Geometric	12
37	.271	.338	Geometric	20
38	.461	.346	20 within 90 feet, 3 from 90-650 feet	23
39	.454	.367	15 within 90 feet, 3 from 90-650 feet	18
40	.448	.374	12 within 90 feet, 3 from 90-650 feet	15
41	.454	.368	12 within 90 feet, 1 from 90-650 feet	13
42	.437	.381	8 within 90 feet, 1 from 90-650 feet	9

FIGURE 1

5 OR 9 SPOT PATTERN GRIDS

• GRID BLOCK CENTERS
O INJECTION WELL
● PRODUCTION WELL

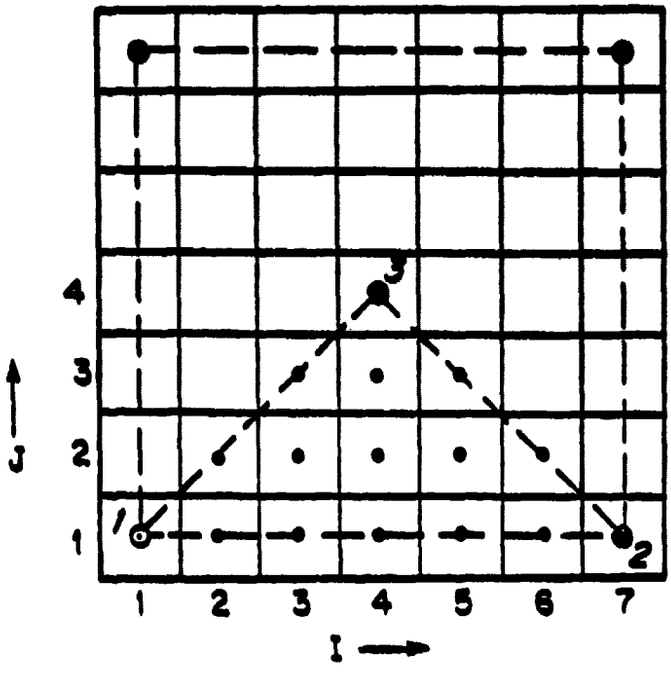

1A. PARALLEL GRID

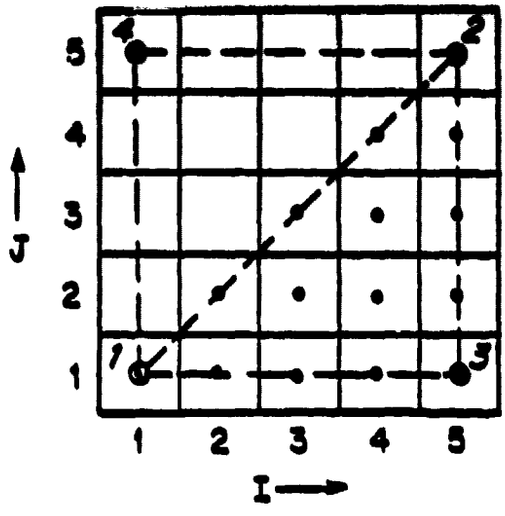

1 B. DIAGONAL GRID

FIGURE 2

7-SPOT PATTERN GRIDS

- • GRID BLOCK CENTERS
- O INJECTION WELL
- ● PRODUCTION WELL

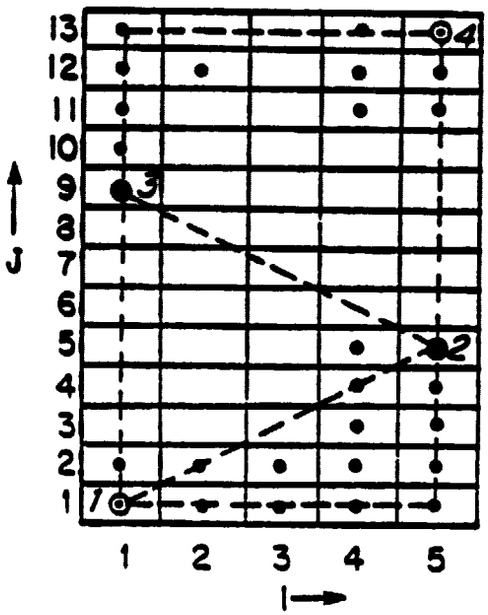

2A. 1/2 7-SPOT GRID

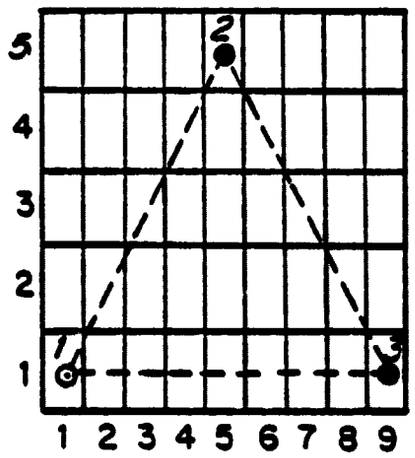

2B. 1/6 7-SPOT GRID

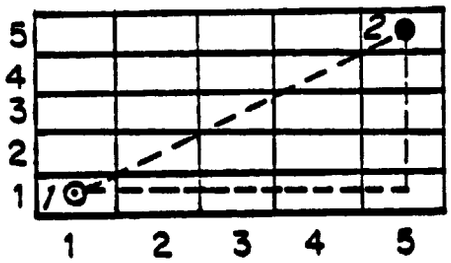

2C. 1/12 7-SPOT GRID

FIGURE 3
GRID ORIENTATION EFFECT UPON OIL PRODUCTION RATE IN 1/8 OF 5-SPOT: 5-POINT VS. 9-POINT

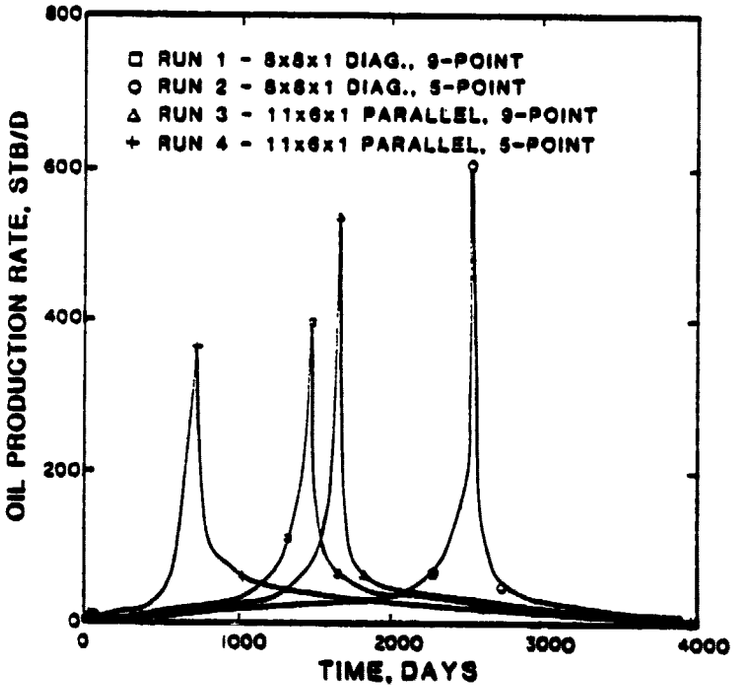

FIGURE 4
EFFECT OF GRID ORIENTATION UPON CUMULATIVE OIL RECOVERY IN 1/8 OF 5-SPOT: 5-POINT VS. 9-POINT

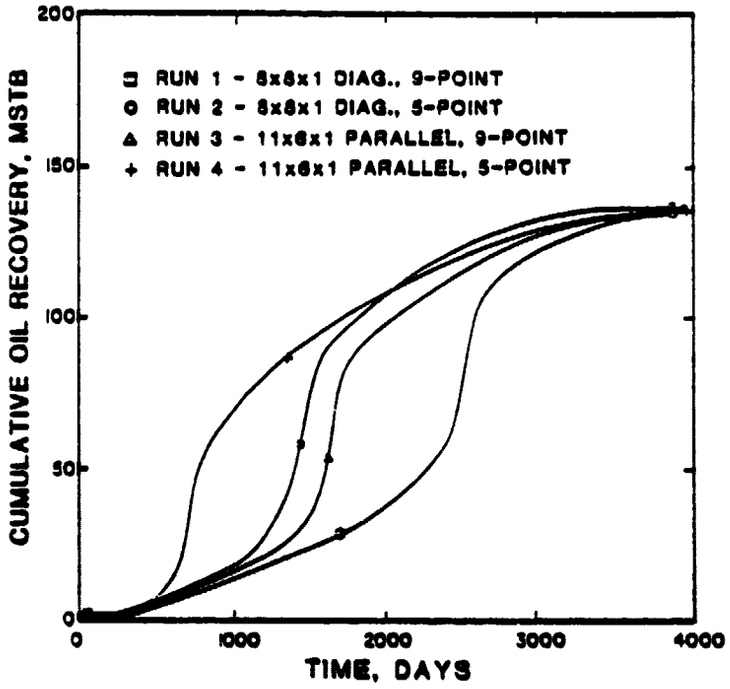

FIGURE 5
GRID ORIENTATION EFFECT UPON FAR & NEAR WELL PRODUCTION IN 1/8 OF 9-SPOT, 5-POINT DIFFERENCE

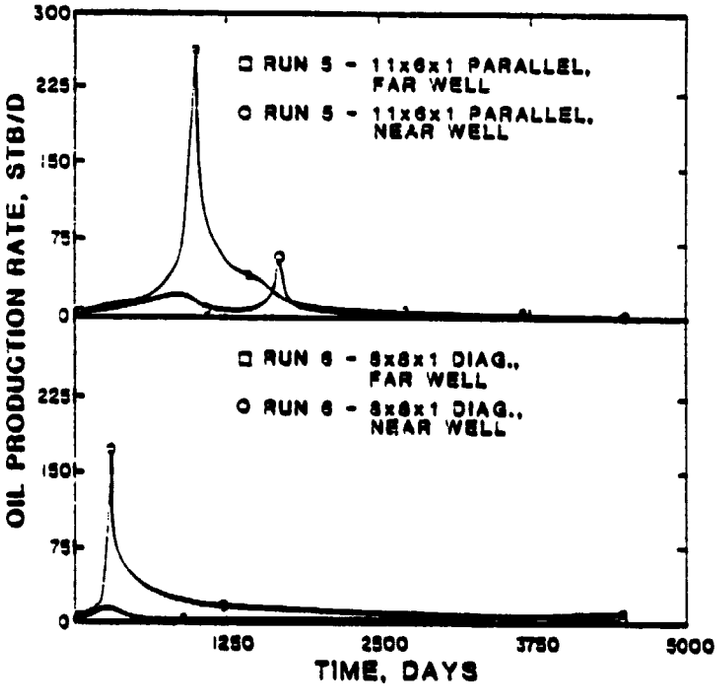

FIGURE 6
GRID ORIENTATION EFFECT UPON CUMULATIVE OIL RECOVERY IN 1/8 OF 9-SPOT, 5-POINT DIFFERENCE

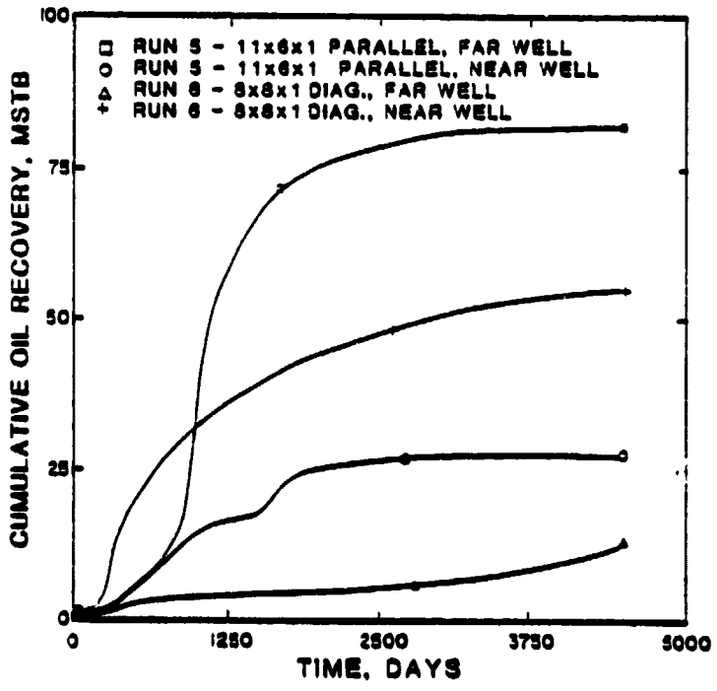

FIGURE 7
GRID ORIENTATION EFFECT UPON OIL PRODUCTION RATE IN 1/8 OF 9-SPOT, 9-POINT DIFFERENCE

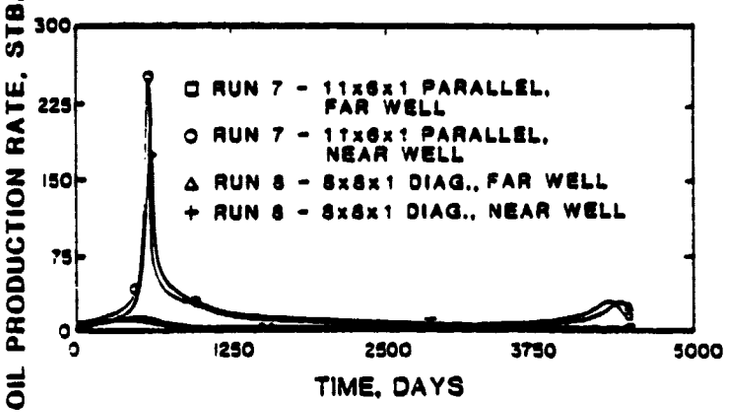

FIGURE 8
GRID ORIENTATION EFFECT UPON CUMULATIVE OIL RECOVERY IN 1/8 OF 9-SPOT, 9-POINT DIFFERENCE

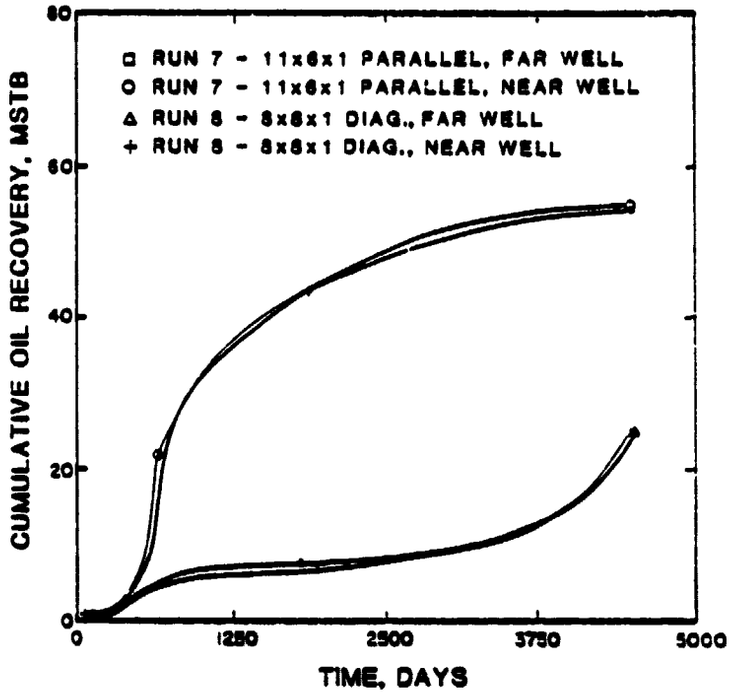

FIGURE 9
1/8 5-SPOT

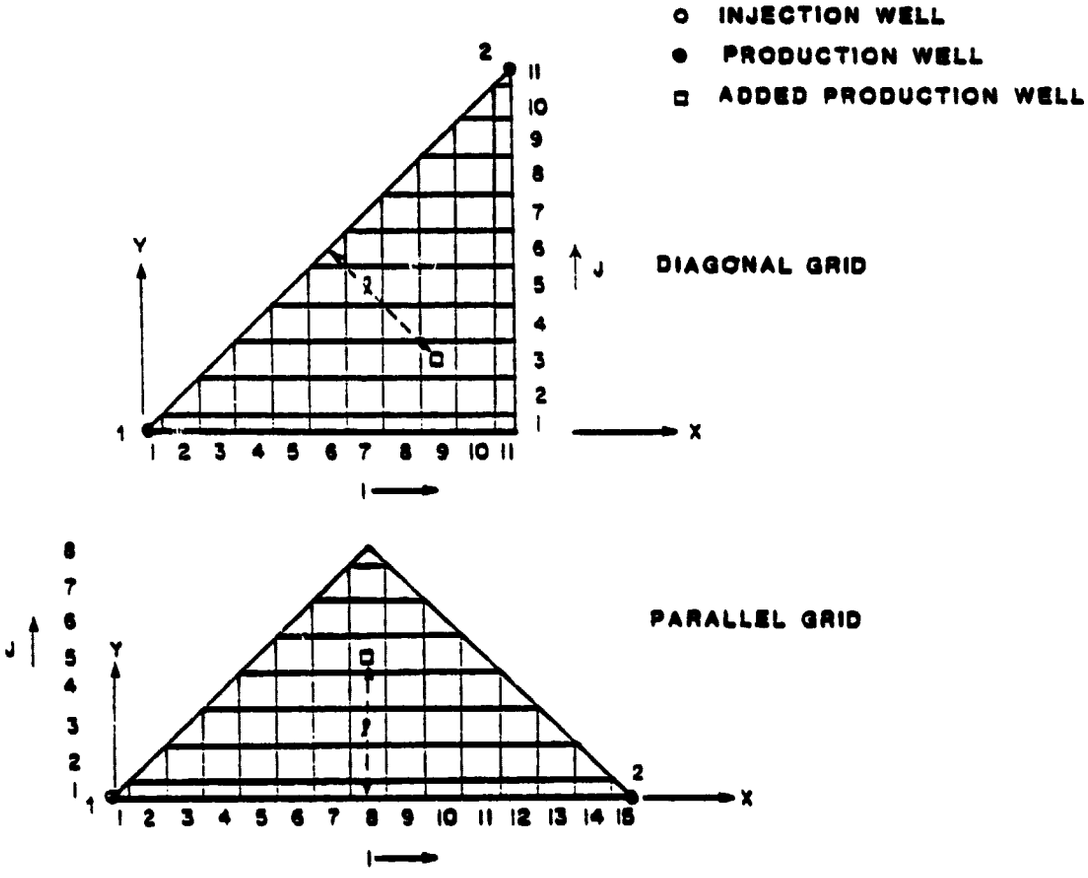

FIGURE 10
GRID ORIENTATION EFFECT UPON CUMULATIVE OIL RECOVERY IN 1/8 5-SPOT WITH ADDED PRODUCER

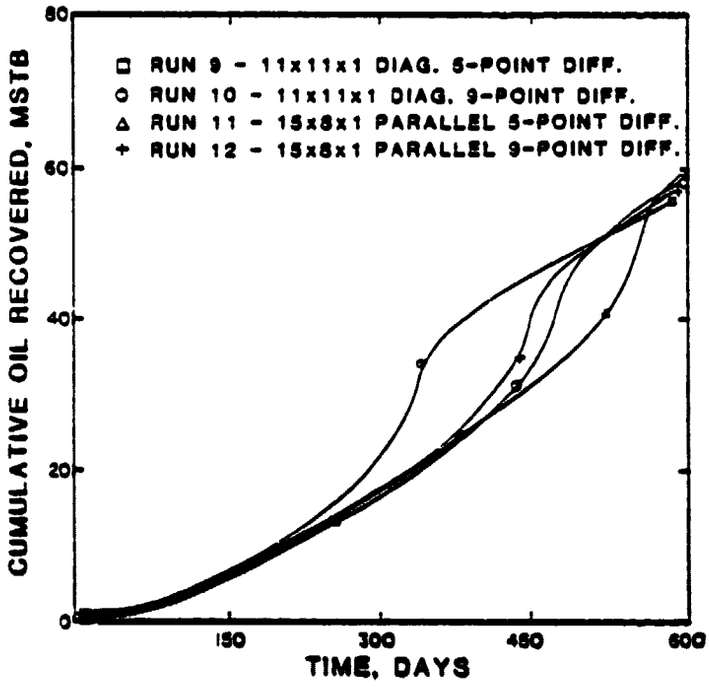

FIGURE 11
GRID ORIENTATION EFFECT UPON OIL PRODUCTION RATE IN 1/8 5-SPOT WITH ADDED PRODUCER

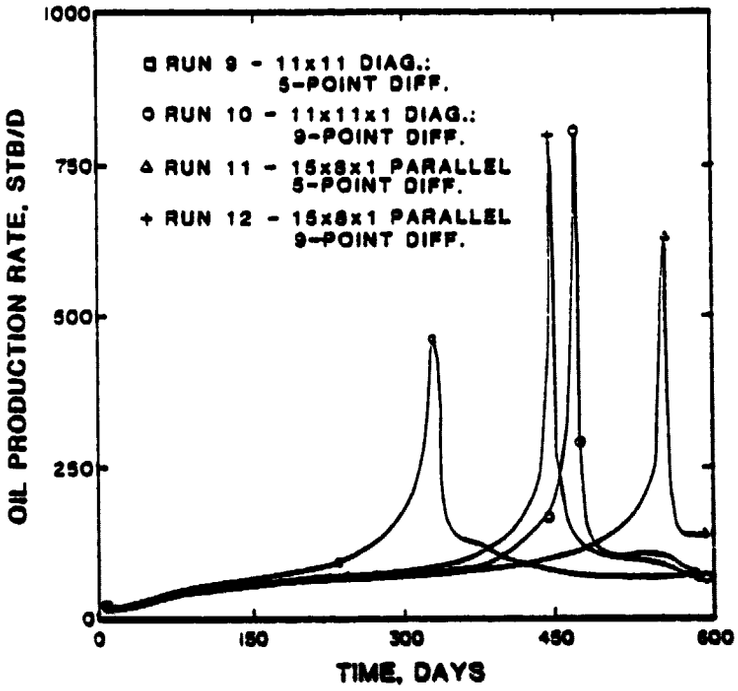

FIGURE 12
GRID ORIENTATION EFFECT UPON CUMULATIVE OIL RECOVERY IN 1/4 OF 9-SPOT, 9-POINT DIFFERENCE

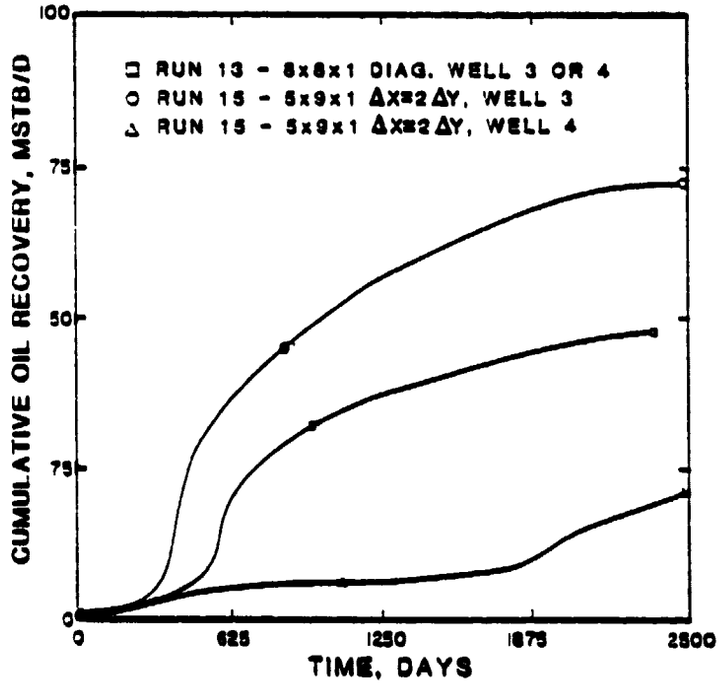

FIGURE 13
GRID ORIENTATION EFFECT UPON TOTAL LIQUID PRODUCTION RATE IN 1/4 OF 9-SPOT, 9-POINT DIFFERENCE

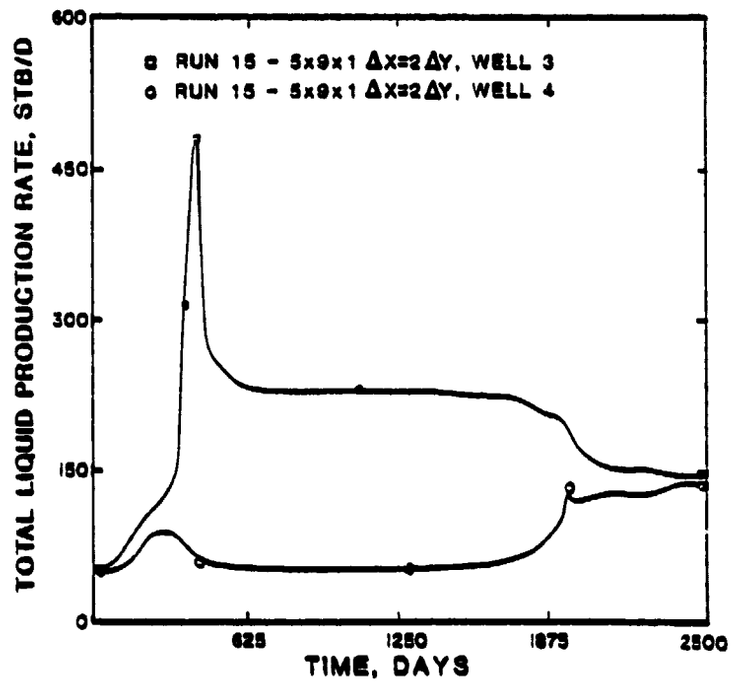

FIGURE 14
GRID ORIENTATION EFFECT UPON CUMULATIVE OIL RECOVERY IN 1/4 OF 9-SPOT, 9-POINT DIFFERENCE

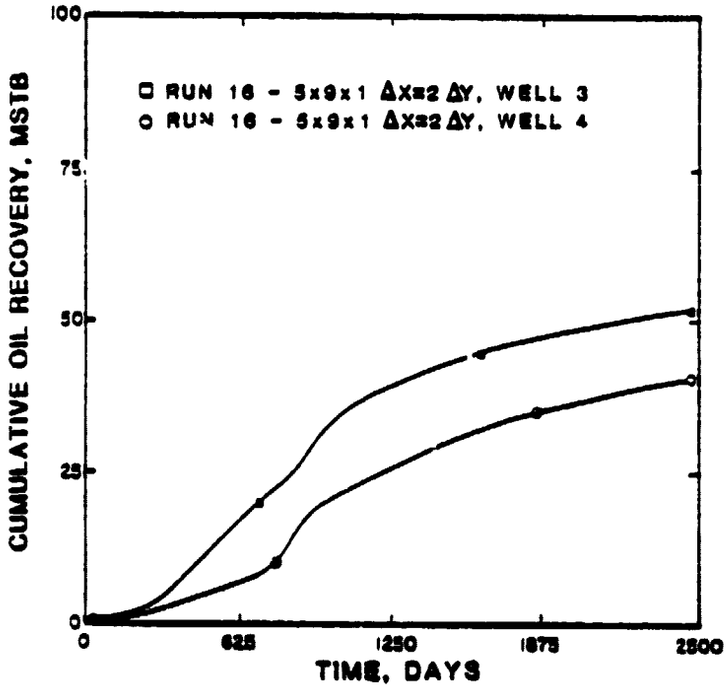

FIGURE 15
GRID ORIENTATION EFFECT UPON CUMULATIVE OIL RECOVERY IN 1/2 AND 1/12 7-SPOT, 5 VS. 9-POINT

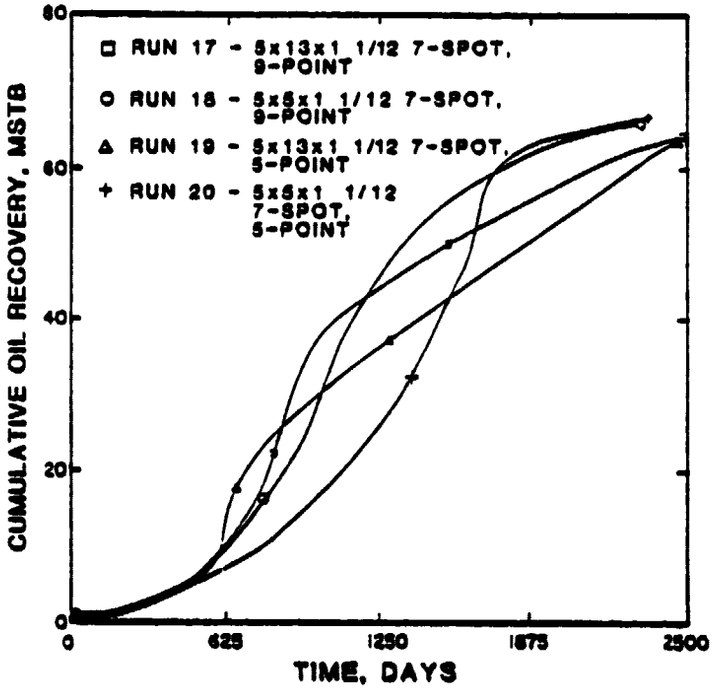

FIGURE 16
GRID ORIENTATION EFFECT UPON OIL RATE & RECOVERY IN 1/6 OF 7-SPOT, 5-POINT DIFFERENCE

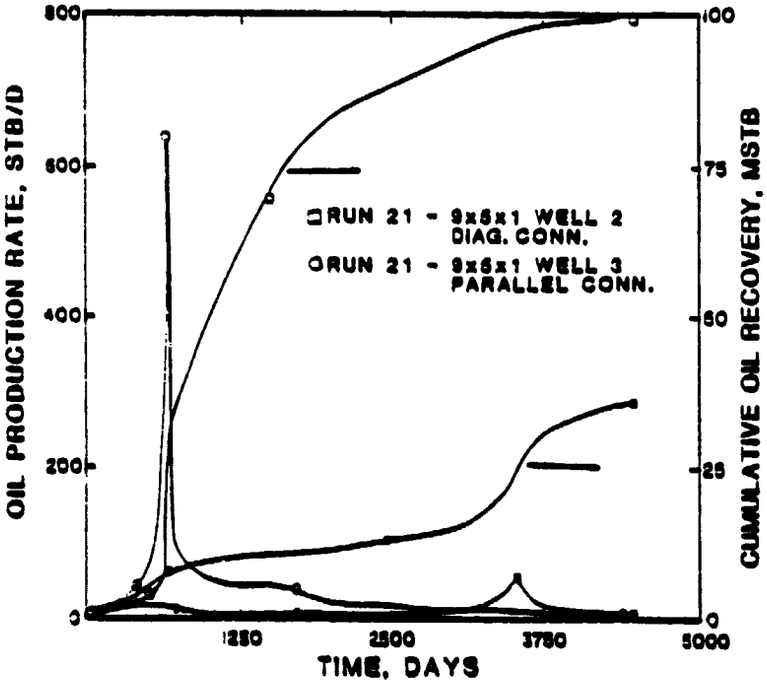

FIGURE 17
GRID ORIENTATION EFFECT UPON OIL RATE & RECOVERY IN 1/6 OF 7-SPOT, 9-POINT DIFFERENCE

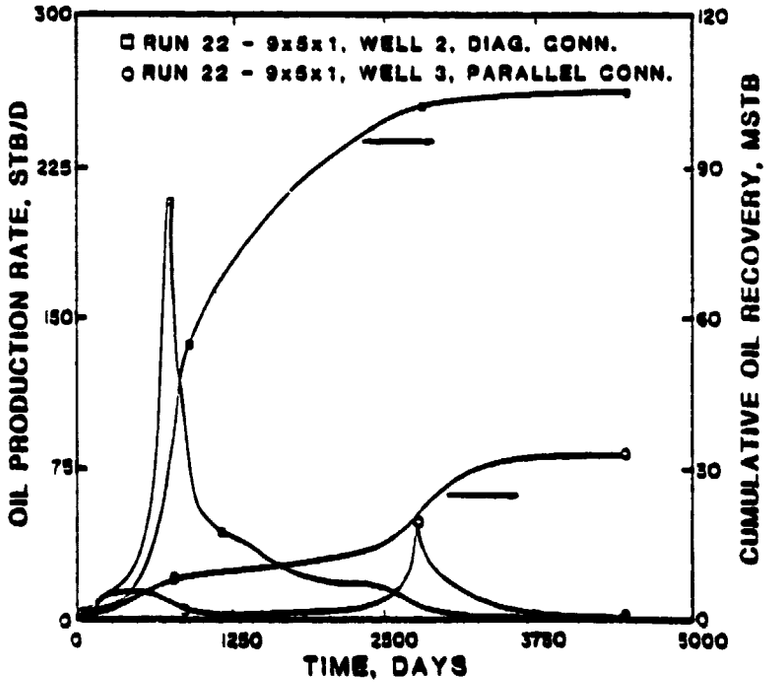

FIGURE 18
GRID ORIENTATION EFFECT UPON OIL RATE & RECOVERY IN 1/6 OF 7-SPOT, 5-POINT DIFFERENCE

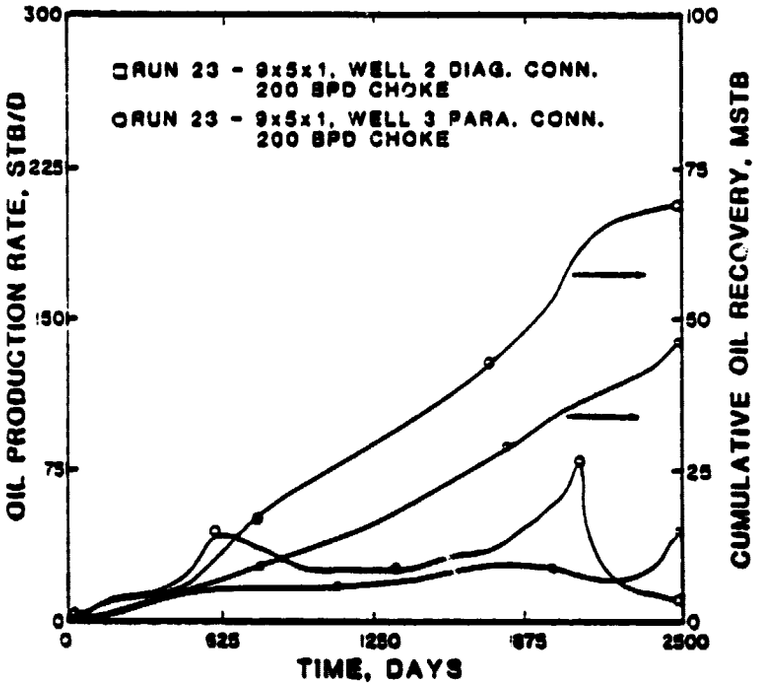

FIGURE 19
GRID ORIENTATION EFFECT UPON OIL RATE & RECOVERY IN 1/6 OF 7-SPOT, 9-POINT DIFFERENCE

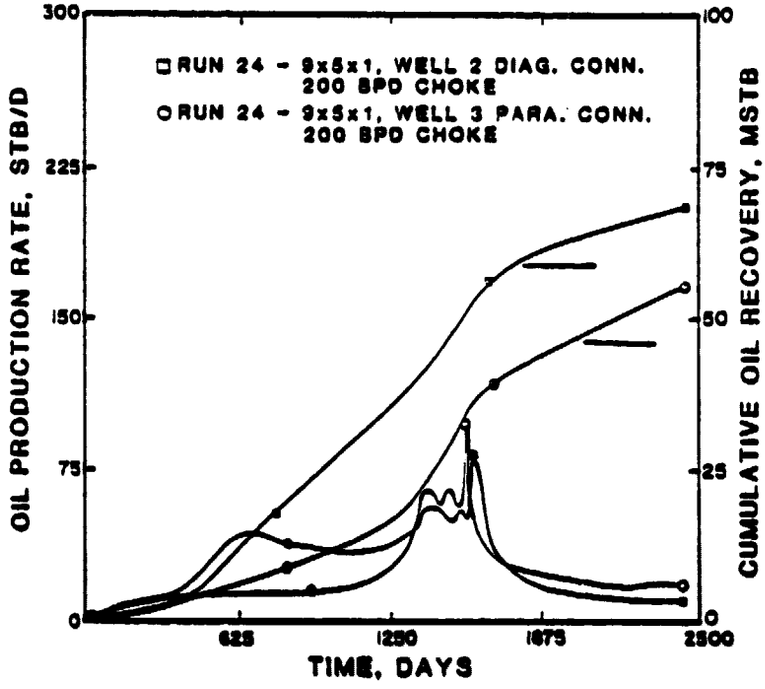

FIGURE 20
EFFECT OF ELIMINATION OF TIP BLOCKS UPON OIL RECOVERY IN 1/8 5-SPOT, 9-POINT DIFFERENCE

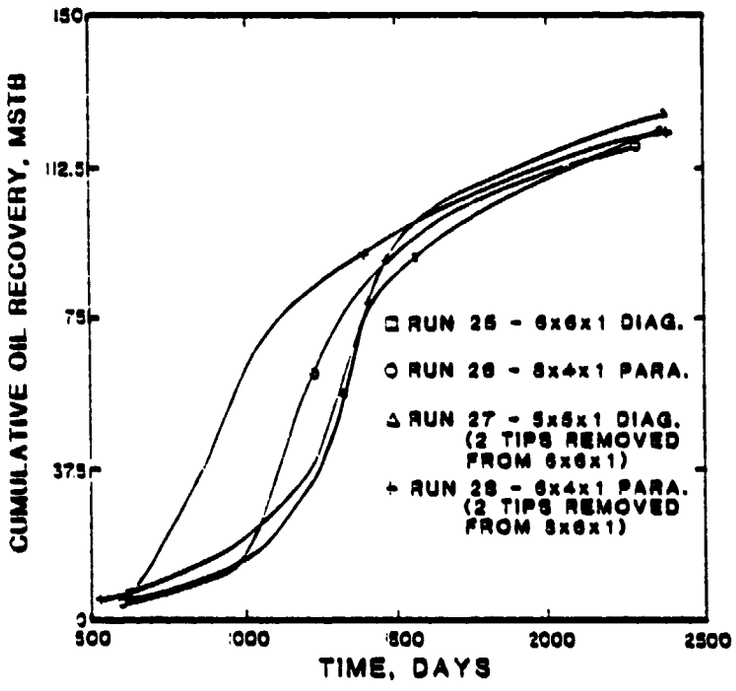

FIGURE 21

DIAGONAL GRID FOR CROSS SECTION

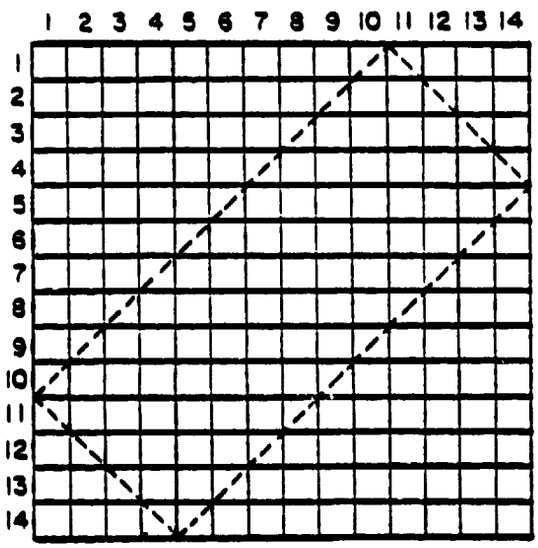

FIGURE 22
GRID ORIENTATION EFFECTS IN
CROSS SECTIONS, ($\omega = .5$ DSMAX = .1)

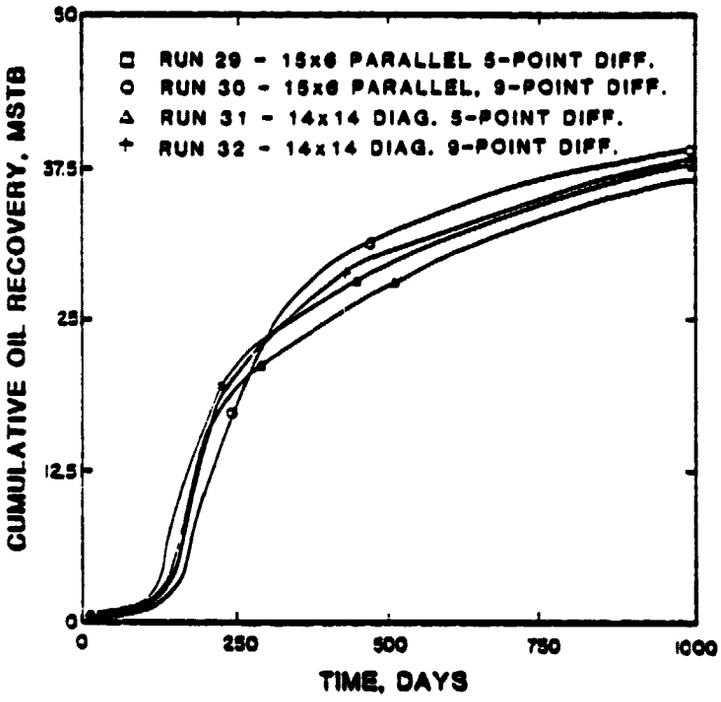

FIGURE 23
EFFECT OF TIME STEP SIZE AND
UPSTREAM WEIGHTING OF CONVECTIVE
HEAT TERM UPON OIL RECOVERY,
5-POINT DIFFERENCE 15x6 PARALLEL

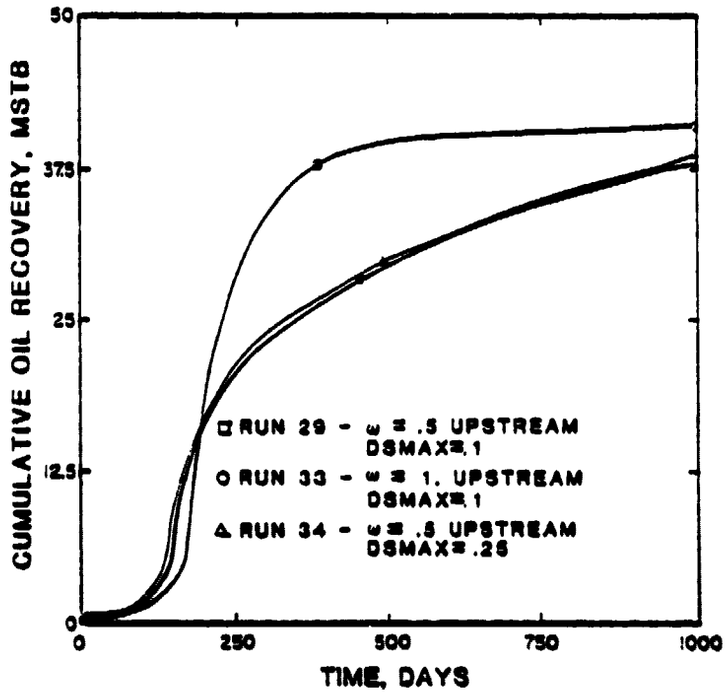

FIGURE 24
SENSITIVITY OF CYCLIC STEAM
TO GRID SPACING EQ-VOL BLOCKS
TO 90 FT, GEOM BLOCKS TO 650 FT

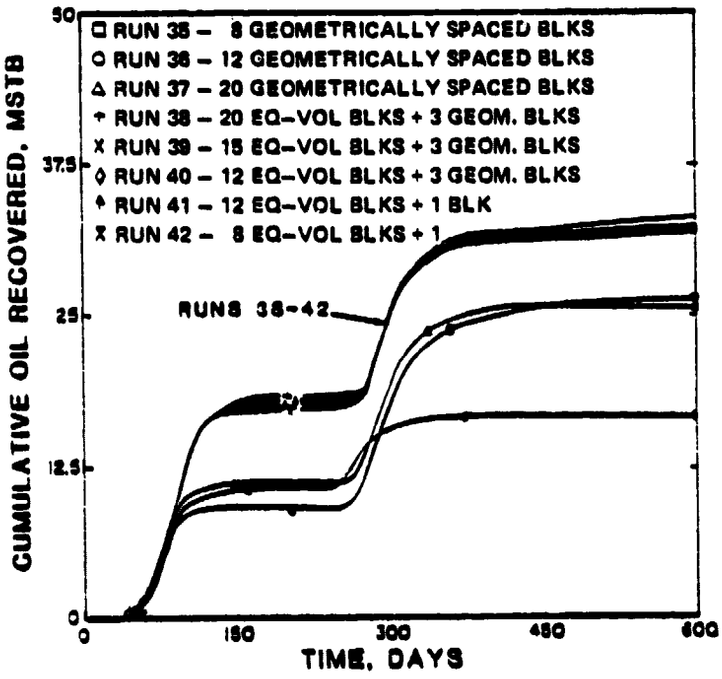

FIGURE 25

CALCULATED PRESSURE AND OIL SATURATION PROFILES

AT END OF SECOND CYCLE INJECTION

RUN 38

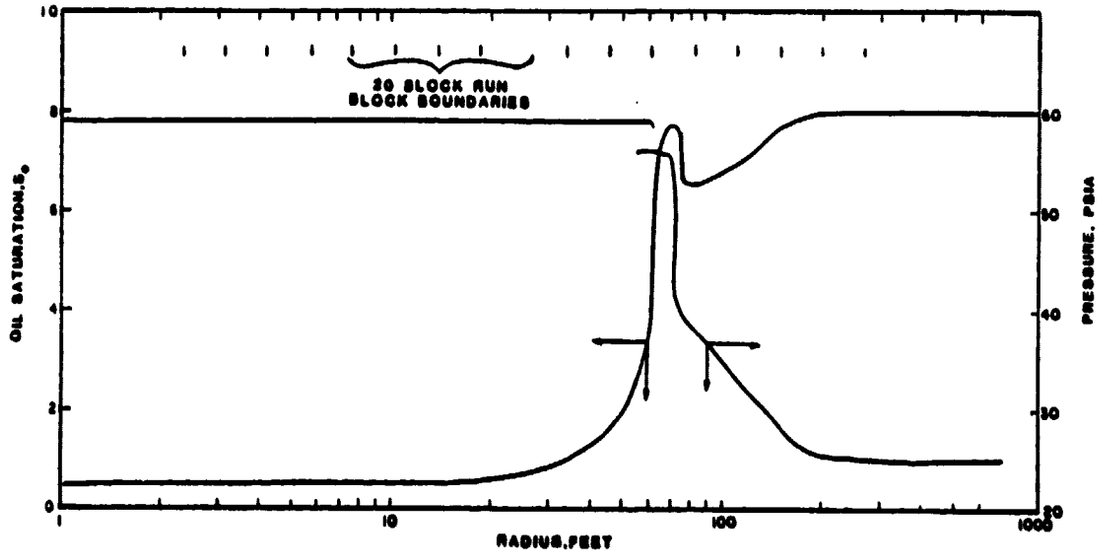

FIGURE 26

COMPARISON OF EQ-VOLUME AND EQUAL-Δr

GRID SPACING IN CYCLIC STEAM SIMULATION